Detection of DNA labeled with magnetic nanoparticles using MgO-based magnetic tunnel junction sensors

Weifeng Shen,[1,a)] Benaiah D. Schrag,[2] Matthew J. Carter,[2] Jin Xie,[3] Chenjie Xu,[3] Shouheng Sun,[3] and Gang Xiao[1,b)]
[1]*Physics Department, Brown University, Providence, Rhode Island 02912, USA*
[2]*Micro Magnetics Inc., 421 Currant Road, Fall River, Massachusetts 02720, USA*
[3]*Chemistry Department, Brown University, Providence, Rhode Island 02912, USA*

(Presented on 6 November 2007; received 13 September 2007; accepted 24 October 2007; published online 5 February 2008)

We have demonstrated the detection of 2.5 μM target DNA labeled with 16 nm Fe_3O_4 nanoparticles (NPs) and 50 nm commercial MACS™ NPs using arrays of magnetic tunnel junction sensors with (001)-oriented MgO barrier layers. Signal-to-noise ratios of 25 and 12 were obtained with Fe_3O_4 and MACS™ NPs, respectively. These data show conclusively that MgO-based MTJ sensor arrays are very promising candidates for future applications involving the accurate detection and identification of biomolecules tagged with magnetic nanoparticles. © *2008 American Institute of Physics*. [DOI: 10.1063/1.2832880]

I. INTRODUCTION

Magnetic nanoparticles have become a powerful and versatile diagnostic tool for biology and nanomedicine.[1] Given their extremely small size and high magnetization, such nanoparticles can be introduced into a living organism, where they can provide a means of monitoring and influencing cellular processes.[2] Once suitably attached, nanoparticles can also be used to transport proteins, nucleic acids, and other biomolecules through microfluidic circuits. In recent years, a sustained effort has been made to design and develop biodetection systems which combine magnetic nanoparticles (NPs) with magnetoresistive (MR) sensors.[3–5] The ultimate goal is to build a high-sensitivity, low-cost, and portable "all-in-one" biodetection system.[6] The principle behind these systems is to specifically attach magnetic nanoparticles to the analyte molecules and then use the MR sensor(s) to detect the stray field generated by the embedded NPs for identification purposes.[7]

The giant magnetoresistance (GMR) and tunneling magnetoresistance (TMR) effects in thin film multilayers have been intensively studied as part of the emerging field of spintronics.[8,9] These technologies have also been widely employed in new types of fully integrated bimolecular recognition assays.[10–12] Compared with GMR sensors, magnetic tunnel junction (MTJ) sensors offer higher magnetoresistance (MR) ratios and therefore higher sensitivity at low fields. In addition, very large magnetoresistance ratios (over 200%) have recently been obtained in MTJ devices using (001)-oriented MgO tunnel barriers.[13,14] These values are nearly an order of magnitude superior to those reported for today's best GMR sensors. As a result, MgO-based MTJs are better suited for the accurate detection of the small magnetic fields (<1 Oe) which are typically encountered in biomagnetic applications. In this paper, we report on the design and development of the first magnetic biosensors based on MTJ sensor arrays with an MgO barrier. We demonstrate the use of these sensor arrays for the detection of 2.5 μM single-strand analyte DNA labeled with 16-nm-diameter Fe_3O_4 NPs and 50 nm commercial MACS™ NPs. These sensor arrays are identical in spot size and in the functionalization process, to commercial DNA microarrays, and have signal and noise characteristics which are superior to those previously reported for single MTJ devices.

II. EXPERIMENT

MTJ multilayer films were deposited on thermally oxidized Si wafers using a custom multitarget high-vacuum magnetron sputtering system (base pressure of 2×10^{-8} Torr). The MTJ stacks used in this study had the following layer structure: (thicknesses in nanometers) substrate/Ta (30)/$Co_{50}Fe_{50}$ (2)/IrMn 15/$Co_{50}Fe_{50}$ (2)/Ru (0.8)/$Co_{40}Fe_{40}B_{20}$ (3)/MgO (1.4)/$Co_{40}Fe_{40}B_{20}$ (3)/Ta (10)/Ru (5). Micron-size elliptical junctions were patterned using standard optical lithography and ion milling. A 100-nm-thick gold layer was deposited over the junction area and patterned into low-resistance electrical contacts for each MTJ. The detailed MTJ sensor fabrication processes which were employed are described in a previous work.[15,16] Figure 1 shows a typical transfer curve of a single MTJ sensor with a 60 Oe external biasing field, showing a MR ratio of 97% and a zero-field junction resistance of 15 Ω. Over the field range of ±10 Oe, a magnetic sensitivity of 0.91%/G is obtained for this sensor.

A novel type of MTJ sensor array was designed to detect the presence of magnetic NPs bonded onto the sensor area. It consists of a number of interconnected MTJ sensors, with adjacent MTJ sensors connected to each other through (alternately) the bottom or top electrical leads. An optical picture of 256 MTJ sensors in a serial array is shown in the inset of Fig. 1. Each individual MTJ sensor has lateral dimensions of 6×18 μm^2 and the sensor array has a total area of 200×200 μm^2. We have chosen the size of this area to be identical to the standard spot size of commercial DNA microar-

[a)]Electronic mail: shen@physics.brown.edu.
[b)]Electronic mail: xiao@physics.brown.edu.

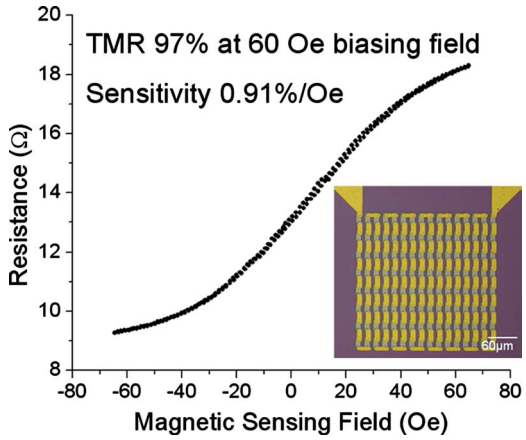

FIG. 1. (Color online) A typical TMR transfer curve of a single MTJ sensor (3×6 μm^2) in a 60 Oe external bias field. Inset: an optical picture of 256 MTJ sensors in a serial array.

ray piezospotter devices. When a layer of magnetic NPs is biologically bonded onto the sensor surface, the MTJ sensor array will generate a total signal proportional to the coverage of NPs, which is in turn related in turn to the concentration of target molecules in the analyte sample.

In order to detect the existence of target molecules (DNA or proteins), the MTJ sensor arrays need to be biologically treated, so as to be able to capture the functionalized nanoparticles. We utilized the following sensor surface treatment steps to accomplish these goals. The sensor surface was passivated with a 100-nm-thick SiO_2 layer and then spin coated with polyethylenimine (PEI) in chloroform solution (about 70 nm in thickness), followed by a 1 min rinse in ethanol. The probe DNA solution (a mixture of 20 μl 49-base single DNA strands and 80 μl phosphate buffered saline, with a *p*H of 10) was introduced by micropipette spotting, followed by incubation in a humid atmosphere at room temperature for 2 h. The sample was then irradiated with 50 mJ of UV light for 30 s, to increase the hybridization efficiency. Prehybridization was done by incubation in 1*M* NaCl and 2.5% polyethylene glycol (PEG) (*p*H 5.0) at 55 °C for 1 h to deactivate unbound epoxy groups. The target DNA solution (containing 20 μl of complementary DNA with biotin at the 3′ end, 50 μl of hybridization buffer, and 30 μl of de-ionized water) was introduced and incubated at 42 °C for 1.5 h, followed by several washing steps to wash away unbound DNA. The sample surface was then neutralized in 1% bovine serium albumin (BSA) solution for 45 min.

Two types of nanoparticles were studied and compared: commercial MACS™ NPs (from Miltenyi Biotec; 50 nm in diameter; M_s=300 emu/cm^3) and Fe_3O_4 NPs synthesized by us (16 nm in diameter; M_s=480 emu/cm^3).[17] Both types of particles are superparamagnetic and both are coated with streptavidin groups during fabrication. We used two different varieties of NPs to ensure that the experimental results are not specific to the type of NP used and to compare the magnetic signal and bonding efficiency of the two types of particles. Through the biotin-streptavidin interaction, these two types of NPs will bond to the biotin-ended target DNA strands when they come into contact with the functionalized sensor surface. For each experiment, a solution containing

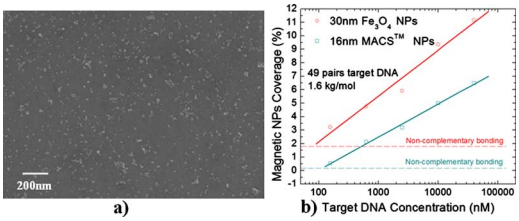

FIG. 2. (Color online) (a) A SEM image showing target DNA and 2.5 μM Fe_3O_4 NPs bonded to the MTJ sensor surface. (b) A semilog graph plotting the coverage of Fe_3O_4 NPs made in-house (red) and MACS™ NPs (dark cyan) vs the concentration of target DNA.

the NPs was introduced to the sensor array via a micropipette. After the NPs have had a chance to bond to the functionalized sensor surfaces, unbound NPs are washed away with a phosphate buffer solution (PBS) buffer solution.

The MTJ sensor array die was then mounted on an open dual-inline socket with a flat surface, so that magnetic nanoparticles could be easily delivered to the sensor surface through a micropipette, without the need for microfluidics. The whole chip was plugged directly into a custom-made printed circuit board designed for the prototyping experiments. A dc biasing field of 50 Oe was applied perpendicular to the sensing axis to reduce the hysteresis of the MTJ sensor array, to make the sensor response more linear, and to increase the field sensitivity.[18] A slowly varying magnetic field was applied along the sensing axis to measure the sensor's MR transfer curves before and after coating with magnetic nanoparticles. This applied field also serves to magnetize the superparamagnetic NPs bonded to the sensor array. As the applied field strength is varied, the NPs bonded to the sensor have an effective dipole moment which is proportional to this field strength. Each dipole moment creates a small added field component (H_{dipole}) at the sensor, which means that it will experience an effective field strength which is slightly smaller than the external applied field, $H_{effect}=H_{applied}-H_{dipole}$, which generates a detectable signal on the MTJ sensor arrays. Because the particles are superparamagnetic and because the applied fields are quite uniform, the NPs do not agglomerate or drift during the experiment.

III. RESULTS AND DISCUSSIONS

In order to quantitatively evaluate the sensor response in the presence of NPs, the relationship between the NP coverage and the concentration of the target DNA needs to be determined. To do this, we first immobilized a 40 μM probe DNA onto the SiO_2/PEI surface, then hybridized it with complementary target DNA at different concentrations, through the same hybridization process as described above. The surfaces of all the samples were examined by scanning electron microscopy (SEM) after the bonding of NPs, as shown in Fig. 2(a). The IMAGE-PRO PLUS® image analysis software was used to count the nanoparticles and calculate the total amount of coverage. Figure 2(b) plots the measured NP coverage as a function of the target DNA concentration. This figure shows that the coverage of both types of NPs is proportional to the logarithm of the concentration of target DNA, which is consistent with results reported by other groups.[5] The 16-nm-diameter Fe_3O_4 NPs showed a better

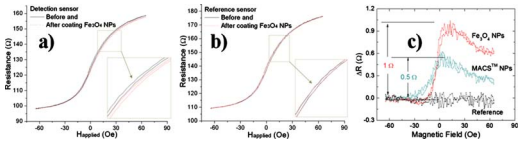

FIG. 3. (Color online) The MR transfer curves measured before and after the bonding of Fe_3O_4 NPs, (a) from an MTJ array treated with DNA and (b) from a nearby array without DNA treatment, meant as a reference. (c) Measured resistance differences for the detection sensors bonded with Fe_3O_4 and MACS™ NPs, respectively, and for the reference sensor.

bonding efficiency than commercial MACS™ NPs, due to their smaller size and the better biochemical treatments used for these NPs. However, Fe_3O_4 NPs also demonstrated a significantly larger nonspecific bonding coverage (1.9%) than MACS™ NPs (0.2%). One reason for this is due to the existence of unwanted adhesion between the Fe_3O_4 particles and the PEI layer.[4]

The detection of target DNA molecules was carried out using a single 64-element MTJ serial array. The sensor array surface was first treated with 40 μM probe DNA, followed by hybridization with a 2.5 μM complementary target DNA. 10 μl of solution containing 16-nm-diameter Fe_3O_4 NPs was then introduced to the sensor area using a handheld precision pipette. About 10 min after the coating of NPs, the sensor surface was washed with PBS buffer to remove nonspecifically bonded NPs. Magnetic response curves of the MTJ array were measured before and after the binding of NPs on the sensor surface. The differences in the two recorded transfer curves are plotted in Fig. 3(a). To further confirm that this magnetoresistance change did indeed result from the binding of Fe_3O_4 NPs, we compared the MR transfer curves measured for a nearby reference MTJ sensor during the same experiment. The reference sensor was located on the same chip but was not biologically treated. Figure 3(b) shows the MR transfer curves from the reference sensor before and after the NPs were introduced, all measured under the same conditions as were used for the active sensor. The essentially identical MR transfer curves of the reference sensor indicate that the resistance changes in the detection sensor are indeed caused by the Fe_3O_4 NPs bonded to the sensor surface through the target DNA molecules.

The resistance variation ΔR of the MTJ array with respect to the initial state is plotted in Fig. 3(c). It can be seen that the maximum deviation in ΔR is $\sim 1\ \Omega$ (0.2 mV) when the sensor array is coated with 16 nm Fe_3O_4 NPs, which corresponds to an average dipole field of $H_{\text{dipole}}=0.16$ Oe applied to the MTJ sensor area. This represents the maximum detected signal for 2.5 μM complementary target DNA strands, according to the bonding between the Fe_3O_4 NPs and the biotin end of the target DNA strands. When using commercial MACS™ NPs, a maximum resistance change (ΔR) of $\sim 0.5\ \Omega$ (corresponding to 0.1 mV of signal and $H_{\text{dipole}}=0.08$ Oe) was observed. These results are consistent with the fact that the Fe_3O_4 NPs show a better bonding efficiency and have a higher magnetic moment than the commercial MACS™ NPs. In contrast, the reference sensor's resistance remained unchanged throughout both experiments. We take the standard deviation of the resistance fluctuations of the reference sensor as an estimate of the system noise level. The measured value is about 0.04 Ω (8 μV). This indicates that for a 2.5 μM concentration of analyte DNA, signal-to-noise ratios of 25 and 12 are estimated for Fe_3O_4 NPs and MACS™ NPs, respectively.

In summary, we have designed and developed MgO-based MTJ serial arrays for the detection of DNA strands labeled with 16 nm Fe_3O_4 NPs and 50 nm MACS™ NPs. We demonstrated the detection of 2.5 μM single-strand DNA after the DNA hybridization process, obtaining signal-to-noise ratios of 25 and 12 when using Fe_3O_4 NPs and MACS™ NPs, respectively. These sensor arrays are identical to conventional DNA microarrays, in terms of function, biological mechanism, and spot size, but offer the advantages of a fully magnetic detection mechanism. Our results also represent the first successful application of MgO-based MTJ devices to this kind of biomagnetic application. The signal-to-noise values which were obtained indicate that MgO-based MTJ arrays hold great promise for the high-sensitivity detection of DNA and/or proteins in the future.

ACKNOWLEDGMENTS

At Brown University, this work was supported by the National Science Foundation (Grant Nos. DMR-0605966 and DMR-0520491) and by DARPA/AFOSR Grant No. F49620-02-1-0307. At Micro Magnetics, Inc., this work was supported by the National Science Foundation (Grant Nos. DMR-0611054). The authors wish to thank Dr. Jan Hoftun, Dr. Xiaoyong Liu, and Mr. Dipanjan Mazumdar for valuable discussions, assistance, and project guidance.

[1] Q. A. Pankhurst, J. Connolly, S. K. Jones, and J. Dobson, J. Phys. D **36**, R167 (2003).
[2] B. Dubertret, P. Skourides, D. J. Norris, V. Noireaux, A. H. Brivanlou, and A. Libchaber, Science **298**, 1759 (2002).
[3] G. Reiss, H. Brueckl, A. Huetten, J. Schotter, M. Brzeska, M. Panhorst, D. Sudfeld, A. Becker, P. B. Kamp, A. Puehler, K. Wojczykowski, and P. Jutzi, J. Mater. Res. **20**, 3294 (2005).
[4] G. X. Li, S. H. Sun, R. J. Wilson, R. L. White, N. Pourmand, and S. X. Wang, J. Am. Ceram. Soc. **126**, 98 (2006).
[5] J. Schotter, P. B. Kamp, A. Becker, A. Puhler, G. Reiss, and H. Bruckl, Biosens. Bioelectron. **19**, 1149 (2004).
[6] M. Piedade, L. A. Sousa, T. M. de Almeida, J. Germano, B. D. da Costa, J. M. Lemos, P. P. Freitas, H. A. Ferreira, and F. A. Cardoso, IEEE Trans. Circuits Syst., I: Regul. Pap. **53**, 2384 (2006).
[7] M. Megens and M. Prins, J. Magn. Magn. Mater. **293**, 702 (2005).
[8] I. Zutic, J. Fabian, and S. Das Sarma, Rev. Mod. Phys. **76**, 323 (2004).
[9] S. A. Wolf, D. D. Awschalom, R. A. Buhrman, J. M. Daughton, S. von Molnar, M. L. Roukes, A. Y. Chtchelkanova, and D. M. Treger, Science **294**, 1488 (2001).
[10] S. X. Wang, S. Y. Bae, G. X. Li, S. H. Sun, R. L. White, J. T. Kemp, and C. D. Webb, J. Magn. Magn. Mater. **293**, 731 (2005).
[11] D. L. Graham, H. A. Ferreira, and P. P. Freitas, Trends Biotechnol. **22**, 455 (2004).
[12] W. F. Shen, X. Y. Liu, D. Mazumdar, and G. Xiao, Appl. Phys. Lett. **86**, 253901 (2005).
[13] S. S. P. Parkin, C. Kaiser, A. Panchula, P. M. Rice, B. Hughes, M. Samant, and S. H. Yang, Nat. Mater. **3**, 862 (2004).
[14] S. Yuasa, T. Nagahama, A. Fukushima, Y. Suzuki, and K. Ando, Nat. Mater. **3**, 868 (2004).
[15] W. F. Shen, D. Mazumdar, X. J. Zou, X. Y. Liu, B. D. Schrag, and G. Xiao, Appl. Phys. Lett. **88**, 182508 (2006).
[16] X. Y. Liu, D. Mazumdar, W. F. Shen, B. D. Schrag, and G. Xiao, Appl. Phys. Lett. **89**, 023504 (2006).
[17] S. H. Sun, Adv. Mater. (Weinheim, Ger.) **18**, 393 (2006).
[18] D. Mazumdar, X. Y. Liu, B. D. Schrag, W. F. Shen, M. Carter, and G. Xiao, J. Appl. Phys. **101**, 09B502 (2007).